RESEARCH ARTICLE SUMMARY

TOPOLOGICAL PHOTONICS

Topological insulator laser: Experiments

Miguel A. Bandres,* Steffen Wittek,* Gal Harari,* Midya Parto, Jinhan Ren, Mordechai Segev,† Demetrios N. Christodoulides,† Mercedeh Khajavikhan†

INTRODUCTION: Physical systems that exhibit topological invariants are naturally endowed with robustness against perturbations, as was recently demonstrated in many settings in condensed matter, photonics, cold atoms, acoustics, and more. The most prominent manifestations of topological systems are topological insulators, which exhibit scatter-free edge-state transport, immune to perturbations and disorder. Recent years have witnessed intense efforts toward exploiting these physical phenomena in the optical domain, with new ideas ranging from topology-driven unidirectional devices to topological protection of path entanglement. But perhaps more technologically relevant than all topological photonic settings studied thus far is, as proposed by the accompanying theoretical paper by Harari *et al.*, an all-dielectric magnet-free topological insulator laser, with desirable properties stemming from the topological transport of light in the laser cavity.

RATIONALE: We demonstrate nonmagnetic topological insulator lasers. The topological properties of the laser system give rise to single-mode lasing, robustness against fabrication defects, and notably higher slope efficiencies compared to those of the topologically trivial counterparts. We further exploit the properties of the active topological platform by assembling topological insulator lasers from *S*-chiral microresonators that enforce predetermined unidirectional lasing even in the absence of magnetic fields.

RESULTS: Our topological insulator laser system is an aperiodic array of 10 unit cell–by–10 unit cell coupled ring resonators on an InGaAsP quantum wells platform. The active lattice uses the topological architecture suggested in the accompanying theoretical paper. This two-dimensional setting is composed of a square lattice of ring resonators coupled to each other by means of link rings. The intermediary links are judiciously spatially shifted to introduce a set of hopping phases, establishing a synthetic magnetic field and two topological band gaps. The gain in this laser system is provided by optical pumping. To promote lasing of the topologically protected edge modes, we pump the outer perimeter of the array while leaving the interior lossy. We find that this topological insulator laser operates in single mode even considerably above threshold, whereas the corresponding topologically trivial realizations lase in multiple modes. Moreover, the topological laser displays a slope efficiency that is considerably higher than that in the corresponding trivial realizations. We further demonstrate the topological features of this laser by observing that in the topological array, all sites emit coherently at the same wavelength, whereas in the trivial array, lasing occurs in localized regions, each at a different frequency. Also, by pumping only part of the topological array, we demonstrate that the topological edge mode always travels along the perimeter and emits light through the output coupler. By contrast, when we pump the trivial array far from the output coupler, no light is extracted from the coupler because the lasing occurs at stationary modes. We also observe that, even in the presence of defects, the topological protection always leads to more efficient lasing compared to that of the trivial counterpart. Finally, to show the potential of this active system, we assemble a topological system based on *S*-chiral resonators, which can provide new avenues to control the topological features.

ON OUR WEBSITE

Read the full article at http://dx.doi.org/10.1126/science.aar4005

CONCLUSION: We have experimentally demonstrated an all-dielectric topological insulator laser and found that the topological features enhance the lasing performance of a two-dimensional array of microresonators, making them lase in unison in an extended topologically protected scatter-free edge mode. The observed single longitudinal-mode operation leads to a considerably higher slope efficiency as compared to that of a corresponding topologically trivial system. Our results pave the way toward a new class of active topological photonic devices, such as laser arrays, that can operate in a coherent fashion with high efficiencies. ■

The list of author affiliations is available in the full article online.
*These authors contributed equally to this work.
†Corresponding author. Email: msegev@techunix.technion.ac.il (M.S.); demetri@creol.ucf.edu (D.N.C.); mercedeh@creol.ucf.edu (M.K.)
Cite this article as M. A. Bandres *et al.*, *Science* **359**, eaar4005 (2018). DOI: 10.1126/science.aar4005

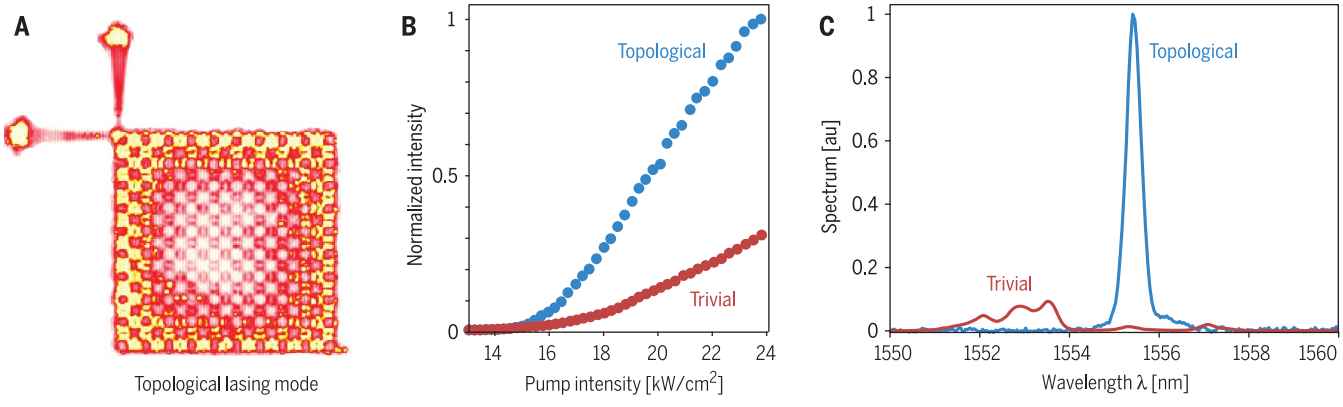

Topological insulator laser. (**A**) Top-view image of the lasing pattern (topological edge mode) in a 10 unit cell–by–10 unit cell array of topologically coupled resonators and the output ports. (**B**) Output intensity versus pump intensity for a topological insulator laser and its trivial counterpart. The enhancement of the slope efficiency is about threefold. Comparing the power emitted in the single mode of the topological array to that of the highest power mode in the trivial array, the topological outperforms the trivial by more than a factor of 10. (**C**) Emission spectra from a topological insulator laser and its topologically trivial counterpart. au, arbitrary units.

RESEARCH ARTICLE

TOPOLOGICAL PHOTONICS

Topological insulator laser: Experiments

Miguel A. Bandres,[1]* Steffen Wittek,[2]* Gal Harari,[1]* Midya Parto,[2] Jinhan Ren,[2] Mordechai Segev,[1]† Demetrios N. Christodoulides,[2]† Mercedeh Khajavikhan[2]†

Physical systems exhibiting topological invariants are naturally endowed with robustness against perturbations, as manifested in topological insulators—materials exhibiting robust electron transport, immune from scattering by defects and disorder. Recent years have witnessed intense efforts toward exploiting these phenomena in photonics. Here we demonstrate a nonmagnetic topological insulator laser system exhibiting topologically protected transport in the cavity. Its topological properties give rise to single-mode lasing, robustness against defects, and considerably higher slope efficiencies compared to the topologically trivial counterparts. We further exploit the properties of active topological platforms by assembling the system from *S*-chiral microresonators, enforcing predetermined unidirectional lasing without magnetic fields. This work paves the way toward active topological devices with exciting properties and functionalities.

Topological insulators are a phase of matter that feature an insulating bulk while supporting conducting edge states (*1*–*3*). Notably, the transport of edge states in topological insulators is granted topological protection, a property stemming from the underlying topological invariants (*2*). For example, in two-dimensional (2D) systems, the ensued one-way conduction along the edge of a topological insulator is, by nature, scatter free—a direct outcome of the nontrivial topology of the bulk electronic wave functions (*3*). Although topological protection was initially encountered in the integer quantum Hall effect (*4*), the field of topological physics developed rapidly after it was recognized that topologically protected transport can also be observed even in the absence of a magnetic field (*5*, *6*). This, in turn, spurred a flurry of experimental activities in a number of electronic material systems (*7*). The promise of robust transport inspired studies in many and diverse fields beyond solid-state physics, such as optics, ultracold atomic gases, mechanics, and acoustics (*8*–*25*). Along these lines, unidirectional topological states were observed in microwave settings (*9*) in the presence of a magnetic field (the electromagnetic analog of the quantum Hall effect), and, more recently, topologically protected transport phenomena have been successfully demonstrated in optical passive all-dielectric environments by introducing artificial gauge fields (*14*, *15*).

[1]Physics Department and Solid State Institute, Technion, Haifa 32000, Israel. [2]CREOL, College of Optics and Photonics, University of Central Florida, Orlando, FL 32816, USA.
*These authors contributed equally to this work.
†Corresponding author. Email: msegev@techunix.technion.ac.il (M.S.); demetri@creol.ucf.edu (D.N.C.); mercedeh@creol.ucf.edu (M.K.)

In photonics, topological concepts could lead to new families of optical structures and devices by exploiting robust, scatter-free light propagation. Lasers, in particular, could directly benefit from such attributes [see the accompanying theoretical paper (*26*)]. In general, laser cavities are prone to disorder, which inevitably arises from fabrication imperfections, operational degradation, and malfunction. Specifically, the presence of disorder in a laser gives rise to spatial light localization within the cavity, ultimately resulting in a degraded overlap of the lasing mode with the gain profile. This implies lower output coupling, multimode lasing, and reduced slope efficiency. These issues become acute in arrays of coupled laser resonators (used to yield higher power), in which a large number of elements is involved. Naturally, it would be of interest to exploit topological features in designing laser systems that are immune to disorder. In this spirit, several groups have recently studied edge-mode lasing in topological 1D Su-Schrieffer-Heeger resonator arrays (*27*–*29*). However, being one-dimensional, they lase in a zero-dimensional defect state, which inherently cannot provide protected transport. Conversely, 2D laser systems can directly benefit from topological protection. Indeed, it was shown theoretically that it is possible to harness the underlying features of topological insulators in 2D laser arrays, when lasing in an extended topological state (*26*, *30*, *31*). As indicated there, such systems can operate in a single-mode fashion with high slope efficiencies, in spite of appreciable disorder. In a following development, unidirectional edge-mode lasing was demonstrated in a topological photonic crystal configuration involving a yttrium iron garnet (YIG) substrate under the action of a magnetic field (*32*). In that system, lasing occurred within a narrow spectral band gap induced by magneto-optic effects. Clearly, it would be of interest to pursue magnet-free approaches that are, by nature, more compatible with fabrication procedures and photonic integration involving low-loss components. In addition, such all-dielectric systems can prove advantageous in substantially expanding the topological band gap and, in doing that, bring the topological protection of photon transport to the level at which lasing is immune to defects and disorder.

Here we report the first observation of topologically protected edge-mode lasing in nonmagnetic,

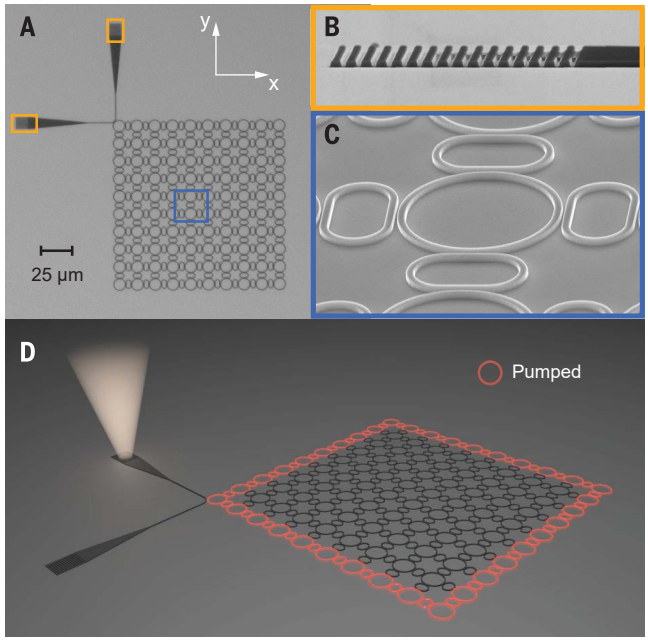

Fig. 1. Topological insulator laser: Lattice geometry. (**A**) Microscope image of an active InGaAsP topological 10 unit cell–by–10 unit cell microresonator array. (**B**) Scanning electron microscopy (SEM) image of the outcoupling grating structures used to probe the array at the orange-outlined locations indicated in (A). (**C**) Magnification of the blue-outlined area indicated in (A), showing a SEM micrograph of a unit cell comprised of a primary ring site surrounded by four identical intermediary racetrack links. (**D**) A schematic of the topological array when pumped along the perimeter to promote lasing of the topological edge mode.

2D topological cavity arrays. We show that this topological insulator laser can operate in single mode, even considerably above threshold, with a slope efficiency that is significantly higher than that achieved in their corresponding trivial realizations. Moreover, we observe experimentally that the topological protection leads to more efficient lasing in the 2D array than in the trivial counterpart, even in the presence of defects. Finally, to show the potential of this active system, we assemble a topological system based on *S*-chiral resonators, which can provide new avenues to control the topological features.

Design of the topological insulator laser

We fabricated a 10 unit cell–by–10 unit cell coupled ring-resonator array on an active platform involving vertically stacked 30-nm-thick InGaAsP quantum wells [see (*33*), Fig. 1A]. We coupled the array to a waveguide that acts as an output coupler, which allowed us to interrogate the system using outcoupling gratings (Fig. 1B, corresponding to the yellow framed regions in Fig. 1A). The active lattice investigated here uses a topological architecture suggested in (*26*), which is based on adding gain and loss to the topological passive silicon platform demonstrated in (*15*). This 2D setting comprises a square lattice of ring resonators, which are coupled to each other through link rings (Fig. 1, A and C). The link rings are designed to be antiresonant to the main ring resonators. In this all-dielectric design, the intermediary links are judiciously spatially shifted along the y axis, with respect to the ring resonators, to introduce an asymmetric set of hopping phases. The phase shift is sequentially increased along the y axis in integer multiples of $\pm 2\pi\alpha$, designed here to be $\alpha = 0.25$, where α is proportional to the equivalent magnetic flux quanta passing through a unit cell. In this way, a round trip along any plaquette (consisting of four rings and four links) results in a total accumulated phase of $\pm 2\pi\alpha$, where the sign depends on the direction of the path along this unit cell. This provides the lattice with a synthetic magnetic field and establishes two topologically nontrivial band gaps. The cross section of each ring (500-nm width and 210-nm height) is designed to ensure single transverse-mode conditions at a wavelength of operation of 1550 nm (*33*). The nominal separation between the ring-resonators and off-resonant links is 150 nm, thus leading to two frequency band gaps, each having a width of 80 GHz (0.64 nm). The spectral size of the two band gaps was obtained by experimentally measuring the frequency splitting (0.8 nm) in a binary system of primary resonators, linked by means of an intermediate racetrack ring [see (*33*), part 9]. To promote protected edge-mode lasing, we optically pumped only the outer perimeter of this array at 1064 nm with 10-ns pulses (Fig. 1D). This was achieved using a set of appropriate amplitude masks [see (*33*), part 1]. The intensity structure of the lasing modes was captured by using an InGaAs infrared camera, and their spectral content was then analyzed by using a spectrometer with an array detector (*33*). In what follows, we compare the features of the topological insulator lasers ($\alpha = 0.25$) with those of their trivial counterparts ($\alpha = 0$) under various conditions.

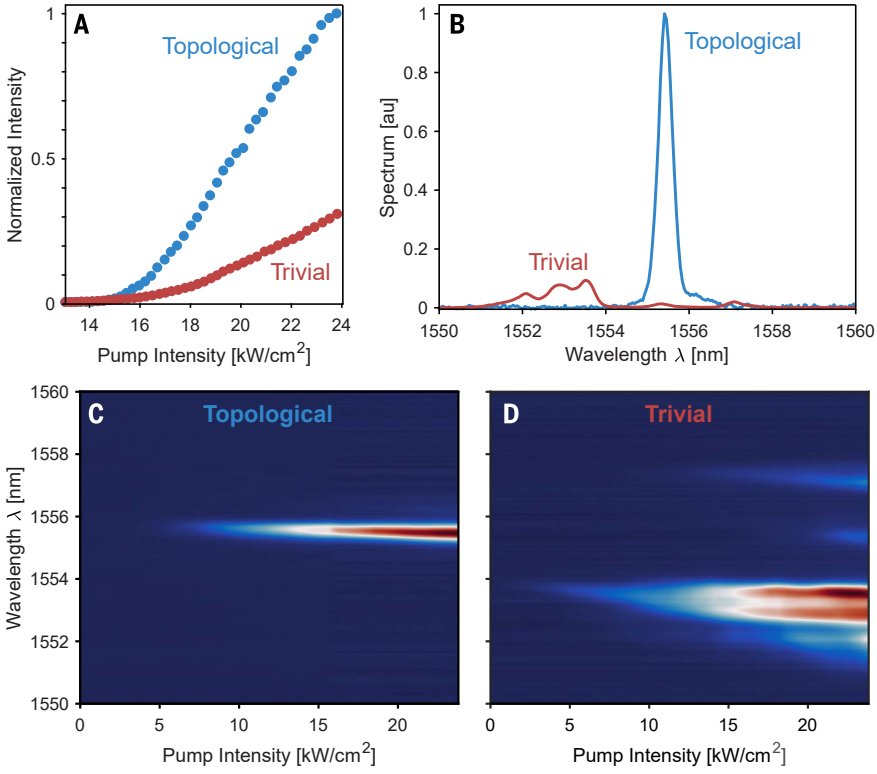

Fig. 2. Slope efficiencies and associated spectra of topological and trivial laser arrays. (**A**) Output intensity versus pump intensity for a 10 unit cell–by–10 unit cell topological array with $\alpha = 0.25$ and its corresponding trivial counterpart ($\alpha = 0$). In this experiment, the enhancement of the slope efficiency is about threefold. (**B**) Emission spectra from a trivial and a topological array when pumped at 23.5 kW/cm^2. au, arbitrary units. (**C** and **D**) Evolution of the spectrum as a function of the pumping intensity for (C) topological and (D) trivial arrays. Single-mode, narrow-linewidth lasing in (C) is clearly evident.

Studying the features of the topological insulator laser

The edge mode can be made to lase by pumping the boundary of the topological array (*26*). In this case, a clear signature of topological lasing would be highly efficient single-mode emission, even at gain values high above the threshold. To observe these features in experiments, we pumped the perimeter of the topological and trivial arrays and measured the lasing output power (integrated over the two outcoupling gratings) and its spectral content. The light-light curves measured for the topological and the trivial arrays (Fig. 2A) clearly show that the topological system lases with a higher efficiency than its trivial counterpart. From their measured spectra (Fig. 2, B and D), we observe that the topological arrays remain single moded over a wide range of pumping densities (Fig. 2C), whereas the trivial arrays (tested over multiple samples) always emit in multiple wavelengths with considerably broader linewidths (Fig. 2D). Importantly, if we only compare the power emitted in the dominant (longitudinal) mode of the topological array to the mode with the highest power in the trivial array, the topological laser outperforms the trivial one by more than an order of magnitude. This difference in performance is attributed to the physical properties of the topological edge modes. The trivial array suffers from several drawbacks. First, the trivial lasing modes extend into the lossy bulk, thus experiencing suppressed emission. Second, the trivial lasing modes try to avoid the output coupler so as to optimize their gain. And finally, because of intrinsic disorder in fabrication, the lasing mode localizes in several different parts of the trivial lattice, each lasing at a different frequency, thereby giving rise to a multimode behavior. Conversely, apart from a weak exponential penetration into the bulk, in topological arrays the edge states are strongly confined to the edge. Moreover, because they are forced to flow around the perimeter, they are always in contact with the output coupler. Finally, because of its inherent topological properties, the lasing edge mode does not suffer from localization, and therefore it uniformly extends around the perimeter (in a single mode), using all the available gain in the system by suppressing any other parasitic mode.

To demonstrate that these active lattices exhibit topological features, we compared their

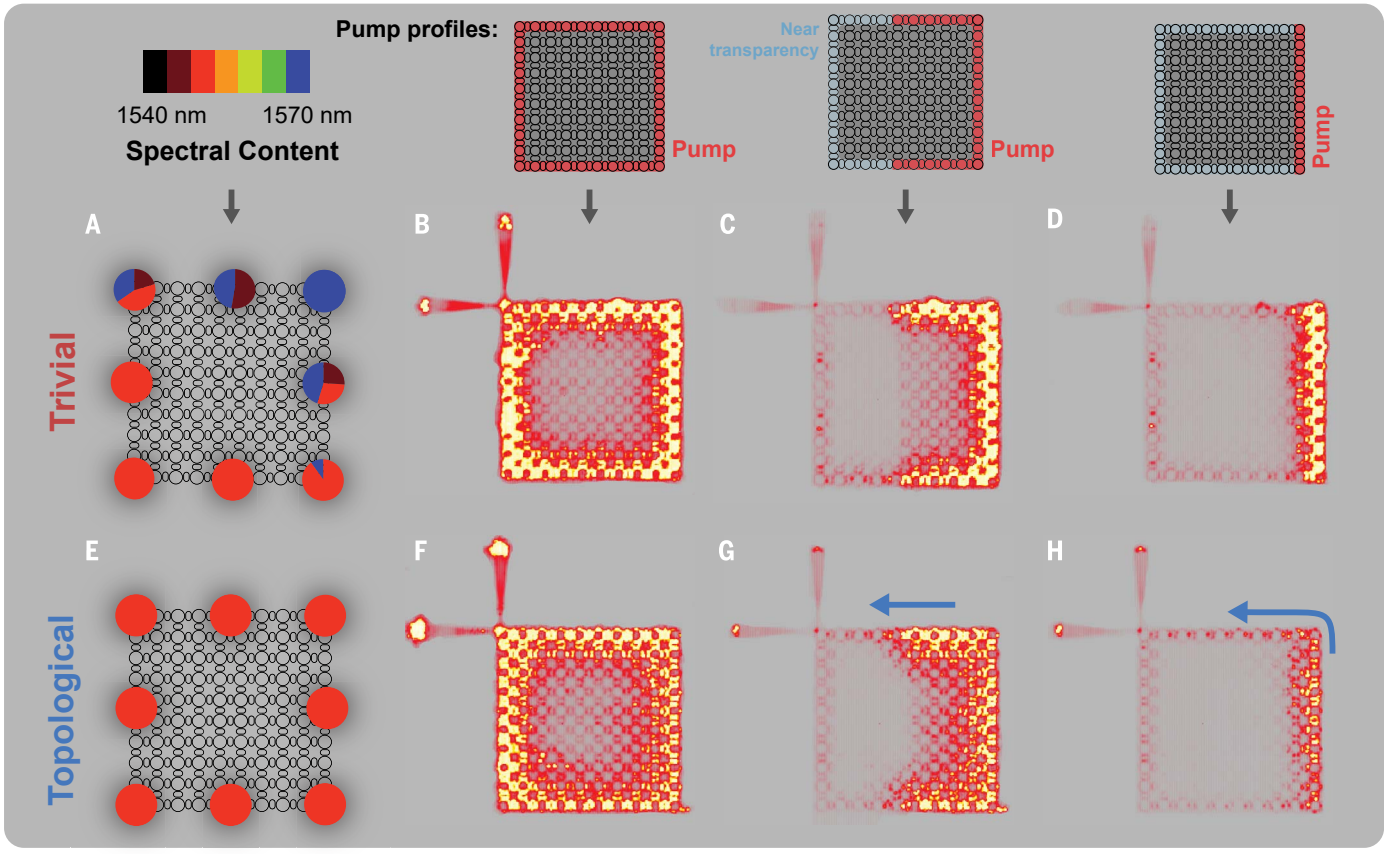

Fig. 3. Lasing characteristics of topological lattices versus those of their corresponding trivial counterparts under several pumping conditions. (**A** to **D**) Trivial and (**E** to **H**) topological lattices. Lasing in a (B) trivial and (F) topological array when their full perimeter is selectively pumped. (A) and (E) represent the spectral content as obtained from specific edge sites of the arrays depicted in (B) and (F), correspondingly. Notice that the topological lattice remains single moded, whereas the trivial one emits in multiple modes. Lasing transport in a (D) trivial array and (H) topological lattice when the right side is pumped. The lasing edge mode in (H) travels (blue arrow) along the unpumped perimeter and exits mostly through the left output grating, whereas the lasing mode in (D) never reaches the output coupler. (C) and (G) present similar results when the pumping region at the right side is further extended into the array. In (G), the lasing edge mode again travels all the way to the output port, whereas the lasing modes of the trivial lattice never reach the extracting ports in (C). This proves that the topological mode travels around the perimeter and always reaches the output port, whereas the lasing modes of the trivial lattice are stationary. The pumping conditions are shown above the labeled panels.

lasing response against that of their trivial counterparts ($\alpha = 0$) when their periphery is pumped. The emission intensity profiles obtained from these two systems are shown in Fig. 3, B and C. To check whether the lasing modes are extended or localized around the perimeter of the lattice, we measured the spectrum of the light emitted from different sites around the arrays (Fig. 3, A and E). For the trivial array, we observed that the spectrum varies around the lattice, with emission occurring over a wide wavelength range, spanning from 1543 to 1570 nm, as shown in Fig. 3A. This is an indication that the trivial array lases in localized domains, each one at a different frequency. By sharp contrast, in the topological array, all sites emit coherently at the same wavelength (Fig. 3E). Such lasing, in a single extended topological edge mode, is a direct manifestation of topologically protected transport. These results are consistent with those presented in Fig. 2. The full spectra of Fig. 3, A and E, are given in (*33*).

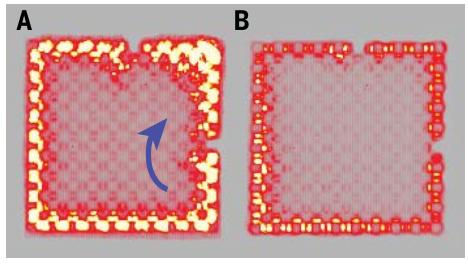

Fig. 4. Robust behavior of the lasing edge mode with respect to defects in a topological array. (**A** and **B**) Lasing response of a (A) topological and (B) trivial array in the presence of two defects intentionally inserted on the periphery, under the same pumping intensity. Note that the edge mode transport in (A) (blue arrow) bypasses the defects, whereas in its trivial counterpart, the lasing occurs from the three separate sections.

Topological transport in these structures was further investigated by selectively pumping the lattice. First, we pumped only one edge of the 2D array, as depicted in Fig. 3D (inset). Under these conditions, the lasing mode in the trivial system is confined to the pumped region (Fig. 3D). In this arrangement, the emission is heavily suppressed both in the bulk as well as along the perimeter, and, consequently, no light is extracted from any of the output grating couplers. By contrast, for the topological array, even when only one side is pumped, the edge mode flows along the periphery, finally reaching the output coupler, as shown in Fig. 3H. In this case, only one output coupler grating emits strongly. This indicates that the lasing mode that reaches the output coupler has a definite chirality in each ring. Given that the emission is in a single mode, one can conclude that lasing takes place in only one topological mode. To show that in the topological case, it is the edge mode that lases,

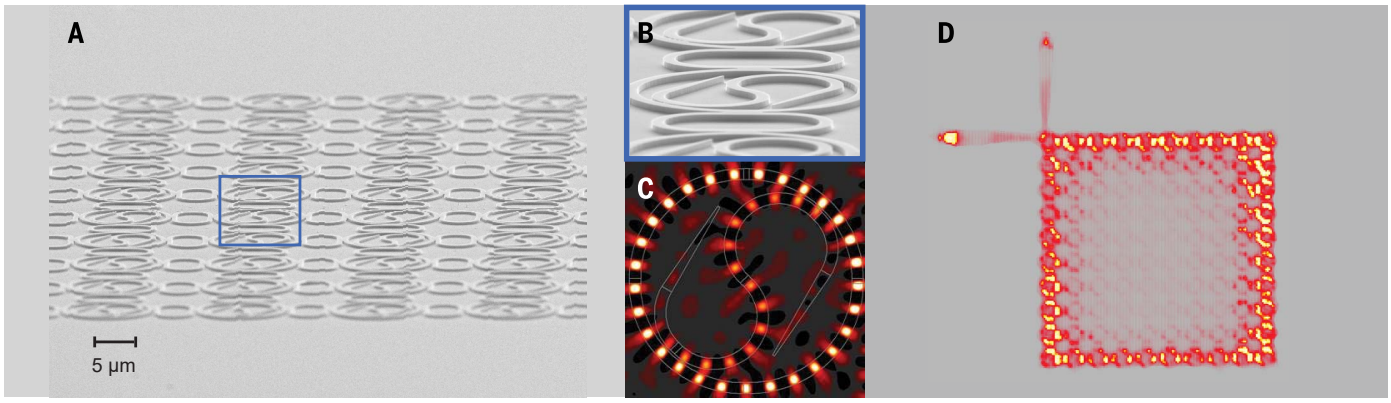

Fig. 5. Topological active array involving chiral *S*-microresonator elements. (**A**) SEM image of a 10 unit cell–by–10 unit cell topological array. The primary resonators feature an internal *S*-bend for enforcing, in this case, a right spin, whereas the intermediate link design is the same as in Fig. 1C. (**B**) A magnification of the SEM micrograph in (A) of the basic elements involved. (**C**) Field distribution in an individual *S*-element, as obtained from finite-difference time-domain simulations. (**D**) Measured intensity profile associated with the lasing edge mode in a topological array with $\alpha = 0.25$. In this system, the perimeter is selectively pumped, and the energy in each ring circulates in a counterclockwise manner, as indicated by the radiation emerging from the extracting ports.

whereas in the trivial case the bulk states lase, we expanded the pumping region at the right edge (Fig. 3C, inset). In the trivial case, even though pumping over a larger area is now provided, still no laser light reaches the output ports (Fig. 3C). This means that there are no traveling edge modes that could reach the output ports. Conversely, for the topological array, the lasing edge mode reaches the output coupler with a fixed chirality within each ring (Fig. 3G). This shows that the topological lasing mode extends around the perimeter and travels all the way to the output ports, whereas the lasing in the trivial case occurs in stationary localized modes. In this vein, we tested multiple samples and found that the same features consistently emerged in a number of different designs (different resonance frequencies, couplings, etc.) in a universal manner. A video showing the behaviors of partially pumped topological and trivial arrays are provided as supplementary materials [see (*33*), part 10] and more features associated with these arrays can be found in [(*33*), parts 3 and 5].

Introducing defects

Next, we studied lasing in a topological structure and in its trivial counterpart, in the presence of defects, which are intentionally introduced into the structures. We removed specific microrings along the perimeter, where pumping is provided (i.e., we remove two gain elements). Figure 4 shows the light emission from these two types of structures. These results demonstrate that in a topological system (Fig. 4A), light is capable of bypassing the defects by penetrating into the bulk and displaying lasing in an extended edge mode of almost uniform intensity. Conversely, the intensity of the emitted light in the trivial structure is considerably suppressed (Fig. 4B), and the defects effectively subdivide the perimeter into separate regions that lase independently (both measurements were performed at identical pump power levels). Hence, the topological insulator laser is robust against defects, even when introduced into the gain regions. [Further evidence of this robustness in the presence of disorder is given in (*33*), part 8.]

Laser based on an array of chiral *S*-bend elements

Having established the underlying concepts of the topological insulator laser and the promise it holds for exploring new aspects of topological physics, specifically in active media, it is interesting to discuss some of the directions to which these ideas can lead. As an example, embarking on fundamental aspects such as Maxwell's reciprocity in the presence of nonlinearity, as well as on potential applications, we modified the individual resonators in the topological insulator laser so as to break the symmetry between the clockwise (CW) and counterclockwise (CCW) modes in each ring. Instead of using conventional rings, we used a special *S*-bend design (*34*) for each primary cavity element in the topological lattice (Fig. 5, A and B). The intermediary links remained the same as in the previous designs (Fig. 1A). In this system, each laser microresonator selectively operates in a single spinlike manner, i.e., in either the CW or the CCW direction, by exploiting gain saturation and energy recirculation among these modes. The *S*-chiral elements involved, in the presence of nonlinearity (gain saturation) and the spatial asymmetry of the *S*-bends, add unidirectionality to the topological protection of transport. In the experiments described in Fig. 5, we observe suppression of more than 12 dB between the right- and left-hand spins in each resonator [see (*33*), part 6]. Finite-difference time-domain simulations also indicate that the differential photon lifetime between the right and left spins in these *S*-bend cavities is about 3 ps, corresponding to an equivalent loss coefficient of 10 cm^{-1} [more details are outlined in (*33*), part 7]. The field distribution in the prevalent spinning mode in these active *S*-resonators is shown in Fig. 5C, featuring a high degree of power recirculation through the *S*-structure that is responsible for the spinlike mode discrimination. The corresponding intensity profile associated with this unidirectional edge-mode energy transport is shown in Fig. 5D. In this case, energy is predominantly extracted from only one of the two outcoupling gratings (with a ~10-dB rejection ratio), which is an indication of unidirectional energy flow in the rings of this topological array.

Discussion

Our all-dielectric topological insulator laser exploits its topological features to enhance the lasing performance of a 2D array of microresonators, making them lase in unison in an extended topologically protected scatter-free edge mode. The observed single longitudinal-mode operation leads to a considerably higher slope efficiency as compared to a corresponding topologically trivial system. The systems described here are based on contemporary fabrication technologies of semiconductor lasers, without need for magnetic units of exotic materials. Our results provide a route for developing a new class of active topological photonic devices, especially arrays of semiconductor lasers, that can operate in a coherent fashion with high slope efficiencies.

REFERENCES AND NOTES

1. D. J. Thouless, M. Kohmoto, M. P. Nightingale, M. Den Nijs, Quantized Hall conductance in a two-dimensional periodic potential. *Phys. Rev. Lett.* **49**, 405–408 (1982). doi: 10.1103/PhysRevLett.49.405
2. M. Hasan, C. Kane, Colloquium: Topological insulators. *Rev. Mod. Phys.* **82**, 3045–3067 (2010). doi: 10.1103/RevModPhys.82.3045
3. X.-L. Qi, S.-C. Zhang, Topological insulators and superconductors. *Rev. Mod. Phys.* **83**, 1057–1110 (2011). doi: 10.1103/RevModPhys.83.1057
4. K. V. Klitzing, G. Dorda, M. Pepper, New method for high-accuracy determination of the fine-structure constant based on quantized Hall resistance. *Phys. Rev. Lett.* **45**, 494–497 (1980). doi: 10.1103/PhysRevLett.45.494
5. C. L. Kane, E. J. Mele, Quantum spin Hall effect in graphene. *Phys. Rev. Lett.* **95**, 226801 (2005). pmid: 16384250

6. B. A. Bernevig, T. L. Hughes, S.-C. Zhang, Quantum spin Hall effect and topological phase transition in HgTe quantum wells. *Science* **314**, 1757–1761 (2006). doi: 10.1126/science.1133734; pmid: 17170299
7. M. König *et al*., Quantum spin hall insulator state in HgTe quantum wells. *Science* **318**, 766–770 (2007). doi: 10.1126/science.1148047; pmid: 17885096
8. F. D. Haldane, S. Raghu, Possible realization of directional optical waveguides in photonic crystals with broken time-reversal symmetry. *Phys. Rev. Lett.* **100**, 013904 (2008). doi: 10.1103/PhysRevLett.100.013904; pmid: 18232766
9. Z. Wang, Y. Chong, J. D. Joannopoulos, M. Soljačić, Observation of unidirectional backscattering-immune topological electromagnetic states. *Nature* **461**, 772–775 (2009). doi: 10.1038/nature08293; pmid: 19812669
10. L. Lu, J. D. Joannopoulos, M. Soljačić, Topological photonics. *Nat. Photonics* **8**, 821–829 (2014). doi: 10.1038/nphoton.2014.248
11. M. Hafezi, E. Demler, M. Lukin, J. Taylor, Robust optical delay lines via topological protection. *Nat. Phys.* **7**, 907–912 (2011). doi: 10.1038/nphys2063
12. K. Fang, Z. Yu, S. Fan, Realizing effective magnetic field for photons by controlling the phase of dynamic modulation. *Nat. Photonics* **6**, 782–787 (2012). doi: 10.1038/nphoton.2012.236
13. A. B. Khanikaev *et al*., Photonic topological insulators. *Nat. Mater.* **12**, 233–239 (2013). doi: 10.1038/nmat3520; pmid: 23241532
14. M. C. Rechtsman *et al*., Photonic Floquet topological insulators. *Nature* **496**, 196–200 (2013). doi: 10.1038/nature12066; pmid: 23579677
15. M. Hafezi, S. Mittal, J. Fan, A. Migdall, J. M. Taylor, Imaging topological edge states in silicon photonics. *Nat. Photonics* **7**, 1001–1005 (2013). doi: 10.1038/nphoton.2013.274
16. L. Tarruell, D. Greif, T. Uehlinger, G. Jotzu, T. Esslinger, Creating, moving and merging Dirac points with a Fermi gas in a tunable honeycomb lattice. *Nature* **483**, 302–305 (2012). doi: 10.1038/nature10871; pmid: 22422263
17. M. Atala *et al*., Direct measurement of the Zak phase in topological Bloch bands. *Nat. Phys.* **9**, 795–800 (2013). doi: 10.1038/nphys2790
18. C. L. Kane, T. C. Lubensky, Topological boundary modes in isostatic lattices. *Nat. Phys.* **10**, 39–45 (2013). doi: 10.1038/nphys2835
19. Z. Yang *et al*., Topological acoustics. *Phys. Rev. Lett.* **114**, 114301 (2015). doi: 10.1103/PhysRevLett.114.114301; pmid: 25839273
20. R. Fleury, A. B. Khanikaev, A. Alù, Floquet topological insulators for sound. *Nat. Commun.* **7**, 11744 (2016). doi: 10.1038/ncomms11744; pmid: 27312175
21. Z. Yu, G. Veronis, Z. Wang, S. Fan, One-way electromagnetic waveguide formed at the interface between a plasmonic metal under a static magnetic field and a photonic crystal. *Phys. Rev. Lett.* **100**, 023902 (2008). doi: 10.1103/PhysRevLett.100.023902; pmid: 18232868
22. X. Cheng *et al*., Robust reconfigurable electromagnetic pathways within a photonic topological insulator. *Nat. Mater.* **15**, 542–548 (2016). doi: 10.1038/nmat4573; pmid: 26901513
23. G. Jotzu *et al*., Experimental realization of the topological Haldane model with ultracold fermions. *Nature* **515**, 237–240 (2014). doi: 10.1038/nature13915; pmid: 25391960
24. M. Aidelsburger *et al*., Measuring the Chern number of Hofstadter bands with ultracold bosonic atoms. *Nat. Phys.* **11**, 162–166 (2015). doi: 10.1038/nphys3171
25. A. P. Slobozhanyuk *et al*., Experimental demonstration of topological effects in bianisotropic metamaterials. *Sci. Rep.* **6**, 22270 (2016). doi: 10.1038/srep22270; pmid: 26936219
26. G. Harari *et al*., Topological insulator laser: Theory. *Science* **359**, eaar4003 (2018). doi: 10.1126/science.aar4003
27. P. St-Jean, V. Goblot, E. Galopin, A. Lemaître, T. Ozawa, L. Le Gratiet, I. Sagnes, J. Bloch, A. Amo, Lasing in topological edge states of a 1D lattice. arXiv:1704.07310 [cond-mat.mes-hall] (24 April 2017).
28. M. Parto, S. Wittek, H. Hodaei, G. Harari, M. A. Bandres, J. Ren, M. C. Rechtsman, M. Segev, D. N. Christodoulides, M. Khajavikhan, Complex edge-state phase transitions in 1D topological laser arrays. arXiv:1709.00523 [physics.optics] (2 September 2017).
29. H. Zhao, P. Miao, M. H. Teimourpour, S. Malzard, R. El-Ganainy, H. Schomerus, L. Feng, Topological hybrid silicon microlasers. arXiv:1709.02747 [physics.optics] (8 September 2016).
30. G. Harari *et al*., in *Conference on Lasers and Electro-Optics* (OSA Technical Digest, Optical Society of America, paper FM3A.3, 2016).
31. S. Wittek *et al*., in *Conference on Lasers and Electro-Optics* (OSA Technical Digest, Optical Society of America, paper FTh1D.3, 2017).
32. B. Bahari *et al*., Nonreciprocal lasing in topological cavities of arbitrary geometries. *Science* **358**, 636–640 (2017). doi: 10.1126/science.aao4551; pmid: 29025992
33. Materials and methods are available as supplementary materials.
34. J. P. Hohimer, G. A. Vawter, D. C. Craft, Unidirectional operation in a semiconductor ring diode laser. *Appl. Phys. Lett.* **62**, 1185–1187 (1993). doi: 10.1063/1.108728

ACKNOWLEDGMENTS

Funding: The authors gratefully acknowledge financial support from the Israel Science Foundation, Office of Naval Research (N0001416-1-2640), NSF (ECCS1454531, DMR-1420620, ECCS 1757025), European Commission Non-Hermitian Quantum Wave Engineering (NHQWAVE) project (MSCA-RISE 691209), Air Force Office of Scientific Research (FA9550-14-1-0037), United States–Israel Binational Science Foundation (2016381), German-Israeli Project Cooperation (Deutsch-Israelische Projektkooperation) program, and Army Research Office (W911NF-16-1-0013, W911NF-17-1-0481). M.S. thanks M. Karpovsky and B. Shillman for their support that came at a critical time. **Author contributions:** All authors contributed to all aspects of this work. **Competing interests:** The authors declare no competing interests. **Data and materials availability:** All data needed to evaluate the conclusions in this paper are available in the manuscript and in the supplementary materials.

SUPPLEMENTARY MATERIALS

www.sciencemag.org/content/359/6381/eaar4005/suppl/DC1
Materials and Methods
Figs. S1 to S11
Reference (*35*)
Movies S1 and S2

3 November 2017; accepted 17 January 2018
Published online 1 February 2018
10.1126/science.aar4005

Topological insulator laser: Experiments

Miguel A. Bandres, Steffen Wittek, Gal Harari, Midya Parto, Jinhan Ren, Mordechai Segev, Demetrios N. Christodoulides and Mercedeh Khajavikhan

Science **359** (6381), eaar4005.
DOI: 10.1126/science.aar4005originally published online February 1, 2018

Topological protection for lasers

Ideas based on topology, initially developed in mathematics to describe the properties of geometric space under deformations, are now finding application in materials, electronics, and optics. The main driver is topological protection, a property that provides stability to a system even in the presence of defects. Harari *et al.* outline a theoretical proposal that carries such ideas over to geometrically designed laser cavities. The lasing mode is confined to the topological edge state of the cavity structure. Bandres *et al.* implemented those ideas to fabricate a topological insulator laser with an array of ring resonators. The results demonstrate a powerful platform for developing new laser systems.

Science, this issue p. eaar4003, p. eaar4005